Mass-yield distributions of fission products from photofission of ^{232}Th induced by 45- and 80-MeV bremsstrahlung

H. Naik and A. Goswami
Radiochemistry Division, Bhabha Atomic Research Centre, Mumbai 400085, India

G. N. Kim,[*] M. W. Lee, and K. S. Kim
Department of Physics, Kyungpook National University, Daegu 702-701, Republic of Korea

S. V. Suryanarayana
Nuclear Physics Division, Bhabha Atomic Research Centre, Mumbai 400085, India

E. A. Kim, S. G. Shin, and M.-H. Cho
Division of Advanced Nuclear Engineering, Pohang University of Science and Technology, Pohang 790-784, Republic of Korea
(Received 23 August 2012; published 26 November 2012)

The mass-yield distributions of various fission products in the 45- and 80-MeV bremsstrahlung-induced fission of ^{232}Th have been determined by using a recoil catcher and an offline γ-ray spectrometric technique in the electron linac at the Pohang Accelerator Laboratory, Korea. The mass-yield distributions were obtained from the fission-product yield data using charge-distribution corrections. The peak-to-valley (P/V) ratio, the average value of light mass ($\langle A_{\rm L}\rangle$) and heavy mass ($\langle A_{\rm H}\rangle$), and the average number of neutrons ($\langle \nu\rangle$) in the bremsstrahlung-induced fission of ^{232}Th at different excitation energies were obtained from the mass-yield data. From the present measurements and the existing data from the ^{232}Th(γ,f) reaction and those from the ^{232}Th(n,f) reaction at various energies, the following observations were obtained: (i) The mass-yield distributions in the ^{232}Th(γ,f) reaction at various energies are triple humped, similar to those of the ^{232}Th(n,f) reaction. (ii) The yields of fission products for $A = 133$–134, $A = 138$–139, and $A = 143$–144 and their complementary products in the ^{232}Th(γ,f) reaction are higher than those of other fission products due to the nuclear structure effect. (iii) The yields of symmetric fission products for $A = 133$–134 and their complementary products in the ^{232}Th(γ,f) reaction are lower than those in the ^{232}Th(n,f) reaction, whereas those for $A = 143$–144 and their complementary products are reversed. (iv) The result of increasing of the symmetric product yield causes the decreasing of the peak-to-valley ratio with increasing the excitation energy. However, it is surprising to see that the increasing trends for the symmetric products yields and the decreasing trends for the P/V ratio in the ^{232}Th(γ,f) and ^{232}Th(n,f) reactions are not similar but those in the ^{238}U(γ,f) and ^{238}U(n,f) reactions are similar to each other. (v) The average values of $\langle A_{\rm L}\rangle$, $\langle A_{\rm H}\rangle$, and $\langle \nu\rangle$ at different excitation energies in the ^{232}Th(γ,f) and ^{232}Th(n,f) reactions are similar but those in the ^{238}U(γ,f) and ^{238}U(n,f) reactions are different.

DOI: 10.1103/PhysRevC.86.054607 PACS number(s): 25.85.Jg

I. INTRODUCTION

Studies of the mass and charge distributions in the low-energy fission of actinides provide information about the effect of nuclear-structure and the dynamics of descent from saddle to scission [1,2]. Among the actinides, various fission products of Th and U are of primary interest from the point of view of significant nuclear-structure effect on the mass and charge distributions [1,2]. Besides this, fission of Th isotopes are of more interest from the point of view of its different type of general behavior expected from the systematic and theory, which is called the Th anomaly. Sufficient data on fission yields are available in different compilations [3–7] as well as in the literature for the reactor neutron-induced fission of ^{232}Th [8–10] and ^{238}U [11,12]. The fission yields data in various monoenergetic neutron fissions of ^{232}Th [13–21] and ^{238}U [22–29] is also available in the literature. Similarly, the yields of fission products in the bremsstrahlung-induced fission of ^{232}Th [30–38] and ^{238}U [31–33,39–52] are available over a broad energy range. From the above-mentioned data, it can be observed that the yields of fission products in the neutron- [8–29] and bremsstrahlung-induced [30–52] fissions of ^{232}Th and ^{238}U are higher around mass numbers 133–134, 138–139, and 143–144 and their complementary products depending on the mass of the fissioning systems [11,12]. However, the yield of fission products around mass numbers 133–134 is less pronounced compared to that at mass numbers 143–144 in both neutron- [13–29] and bremsstrahlung-induced [30–52] fissions of ^{232}Th compared with ^{238}U. We also observed that the yields of fission products around mass numbers 133–134 in the 6.44–13.13 MeV [36,38] and 25–70 MeV [33,37] bremsstrahlung-induced fission of ^{232}Th slightly increases from 4% to 5%. On the other hand, the yields of fission products around mass numbers 143–144 in the bremsstrahlung-induced fission of ^{232}Th decrease from 8% at 6.44–13.13 MeV [36,38] to 6% at 25–70 MeV [33,37]. Besides this, it can be seen from the literature data [30–38] that a third peak for the symmetric products

[*]gnkim@knu.ac.kr

is observed in the 6.44–13.13 MeV [36,38], 25–40 MeV [33], and 50–70 MeV [37] bremsstrahlung-induced fission of ^{232}Th. The observation of the third peak of symmetric products in the bremsstrahlung- [30–38] and neutron-induced [8–21] fission of ^{232}Th is interesting in view of probing the potential-energy surface. However, the yields of symmetric fission products are not available within 15–25 MeV, 40–50 MeV, and 70–100 MeV bremsstrahlung-induced fission of ^{232}Th to examine the above aspect.

In view of the above observations, in the present paper, we determine the yields of fission products in the 45- and 80-MeV bremsstrahlung-induced fission of ^{232}Th using a recoil catcher and an offline γ-ray spectrometric technique in the electron linac at Pohang Accelerator Laboratory (PAL), Korea. These data, along with similar data for ^{232}Th(γ,f), ^{232}Th(n,f), ^{238}U(γ,f), and ^{238}U(n,f) over a wide range of energies, are interpreted as the excitation energy and its role on nuclear structure effects.

II. EXPERIMENTAL PROCEDURE

A. Bremsstrahlung production

The 45- and 80-MeV bremsstrahlung beams were produced from a 100-MeV electron linac of the PAL. The details of the electron linac and bremsstrahlung production are described elsewhere [37,53,54]. The bremsstrahlung was produced when a pulsed electron beam hit a 0.1-mm-thick W target with a size of 100 mm × 100 mm. The W target is located 18 cm from the beam-exit window. A thickness of 0.1 mm for the W target was chosen to avoid the production of neutrons. We simulated the bremsstrahlung spectrum corresponding to an incident electron energy using the GEANT4 computer code [55], as is usually done [37,38,46–50].

B. Sample irradiation

A known amount (209.2–270 mg) of ^{232}Th metal foil with a 0.025 mm thickness and with a 0.25 cm^2 area was wrapped with a 0.025-mm-thick aluminum foil with a purity of more than 99.99%. The sample was fixed on a stand in air 12 cm from a tungsten metal foil. The aluminum wrapper foil acts as a catcher for the fission products recoiling out from the surface of the thorium metal foil during the irradiation. Different sets of target assemblies were irradiated for 1.7 and 0.5 hours with the bremsstrahlung energy of 45 and 80 MeV, respectively. The current of the electron beam during irradiation was 15 mA at 3.75 Hz with a beam width of 1.5 μs. The irradiated target assembly was cooled for 10–30 min. Then, the ^{232}Th metal foil and the aluminum catcher were taken out from the irradiated assembly and mounted separately on a Perspex plate (acrylic glass, 1.5 mm thick).

C. γ-ray spectrometer

The γ-ray counting of fission and reaction products was measured by using an energy- and efficiency-calibrated HPGe detector (EG&G ORTEC, GEM-20180-P) coupled to a PC-based 4K channel analyzer. The energy resolution of the HPGe detector was 1.8 keV full width at half maximum (FWHM) at the 1332.5 keV peak of ^{60}Co. The standard source used for the energy and the efficiency calibration was ^{152}Eu, which has γ rays in the energy range of 121.8–1408.0 keV. Therefore, it was used to avoid the complexity of using so many other standards with one or few γ lines in each. The dead time of the detector system during counting always was kept less than 10% by placing the sample at a suitable distance to avoid pileup effects. The γ-ray counting of the irradiated sample was done in live-time mode and was followed as a function of time for at least three half-lives for major fission products except for ^{95}Zr, ^{141}Ce, and ^{144}Ce.

III. DATA ANALYSIS

A. Determination of excitation energy

The average excitation energy $[\langle E^*(E_e)\rangle]$ of the fissioning nuclei can be obtained by using the following relation [46]:

$$\langle E^*(E_e)\rangle = \frac{\int_0^{E_e} E\, N(E_e, E_\gamma)\sigma_F(E_\gamma)dE_\gamma}{\int_0^{E_e} N(E_e, E_\gamma)\sigma_F(E_\gamma)dE_\gamma}, \tag{1}$$

where $N(E_e, E_\gamma)$ is the number of photons with an energy E_γ produced from the incident electron energy E_e, and $\sigma_F(E_\gamma)$ is the fission cross section as a function of the photon energy (E_γ). The bremsstrahlung spectrum $N(E_e, E_\gamma)$ corresponding to an incident electron energy (E_e) was calculated using the GEANT4 computer code [55]. The photofission cross sections of ^{232}Th in the sub-barrier region [56] and in the energy range of 5–18.3 MeV [57,58] are available. The available data on the photofission cross sections of ^{232}Th are inconsistent [52,55–57]. Thus, the photofission cross section of ^{232}Th as a function of photon energy was calculated using the TALYS computer code version 1.2 [59].

In Eq. (1), the value of $N(E_e,E_\gamma)$ from the GEANT4 code [53] and $\sigma_F(E_\gamma)$ from the TALYS code [59] were used to calculate the average excitation energy. The average excitation energies for the 45- and 80-MeV bremsstrahlung-induced fission of ^{232}Th were found to be 16.95 and 22.49 MeV, respectively.

B. Determination of yields for fission products

The photopeak areas of different γ rays of the fission products of interest were obtained by subtracting the linear Compton background from their net peak areas. From the observed number of γ rays $(N_{\rm obs})$ under the photopeak of an individual fission product, their cumulative yields $(Y_{\rm R})$ relative to ^{135}I were calculated by using the standard decay equation [37,38],

$$Y_{\rm R} = \frac{N_{\rm obs}\,(T_{\rm CL}/T_{\rm LT})\,\lambda}{\left[\int_{E_b}^{E_e} n\,\sigma_F(E)\,\phi(E)dE\right] I_\gamma\,\varepsilon\,(1-e^{-\lambda t_{\rm irr}})e^{-\lambda t_{\rm cool}}(1-e^{-\lambda CL})}, \tag{2}$$

where n is the number of target atoms and $\sigma_F(E)$ is the photofission cross section of the target nuclei in the bremsstrahlung spectrum with an end-point energy of 45 and 80 MeV. Here, $\phi(E)$ is the photon flux from the fission barrier (E_b) [60] to the end-point energy (E_e). I_γ is the branching ratio or intensity of the γ ray, ε is the detection efficiency of the γ rays in the detector system, and λ is the decay constant of the fission-product nuclide of interest ($\lambda = \ln 2/T_{1/2}$). $t_{\rm irr}$ and $t_{\rm cool}$ are the irradiation and cooling times, whereas, $T_{\rm CL}$ and $T_{\rm LT}$ are the real time and the live time of counting, respectively. The nuclear spectroscopic data, such as the γ-ray energies, the half-lives ($T_{1/2}$), and the branching ratios of the fission products were taken from the literature [61,62]. The cumulative yields ($Y_{\rm R}$) of the fission products relative to the fission-rate monitor ^{135}I were calculated using Eq. (2). From the relative cumulative yields ($Y_{\rm R}$) of the fission products, their relative mass-chain yields (Y_A) were calculated by using Wahl's prescription of charge distribution [4]. According to this, the fractional cumulative yield ($Y_{\rm FCY}$) of a fission product in an isobaric mass chain is given as

$$Y_{\rm FCY} = \frac{Q_{\rm EOF}^{a(Z)}}{\sqrt{2\pi\sigma_z^2}} \int_{-\infty}^{Z+0.5} \exp\left[-(Z-Z_{\rm P})^2/2\sigma_z^2\right] dZ, \quad (3)$$

$$Y_A = Y_{\rm R}/Y_{\rm FCY}, \quad (4)$$

where $Z_{\rm P}$ is the most probable charge and σ_z is the width parameter of an isobaric-yield distribution. $Q_{\rm EOF}^{a(Z)}$ is the even-odd effect with $a(Z) = +1$ for even-Z nuclides and -1 for odd-Z nuclides.

From the above equation, it is evident that, in an isobaric mass chain, it is necessary to have knowledge of $Z_{\rm P}$, σ_z, and $Q_{\rm EOF}^{a(Z)}$ to calculate the $Y_{\rm FCY}$ value of a fission product and a mass-chain yield. The $Z_{\rm P}$, σ_z, and $Q_{\rm EOF}^{a(Z)}$ values can be obtained from the fission-yield data of ^{232}Th in the 6.5–14 MeV bremsstrahlung endpoint energy [63]. On the other hand, there are systematic data on the charge distribution in the 6.1–11 MeV [64] and 12–30 MeV [65] bremsstrahlung-induced fission of ^{235,238}U. From these data, it can be seen that the average width parameter ($\langle\sigma_z\rangle$) increases from 0.56 $\pm$ 0.06 at bremsstrahlung energy of 6.1–11 MeV to 0.72 $\pm$ 0.06 at 20–30 MeV. However, there are no data available for the bremsstrahlung-induced fission of ^{232}Th in the 20–30 MeV or higher energy. In view of this, in the present work we have used the average width parameter ($\langle\sigma_z\rangle$) of 0.7. This is justified from the point of average value of 0.70 $\pm$ 0.06 in medium-energy fission shown by Umezawa *et al.* [66].

The $Z_{\rm P}$ values of individual mass chain (A) for the above fission systems were calculated using the prescription of Umezawa *et al.* [66] based on the following relation:

$$Z_{\rm P} = \eta Z_{\rm F} \pm \Delta Z_{\rm P}, \quad \eta Z_{\rm F} = Z_{\rm UCD} = (Z_{\rm F}/A_{\rm F})(A + \upsilon_{\rm post}), \quad (5a)$$

$$\eta = (A + \upsilon_{\rm post})/(A_{\rm C} - \upsilon_{\rm pre}), \quad A_{\rm F} = A_{\rm C} - \upsilon_{\rm pre}, \quad (5b)$$

where $Z_{\rm C}$ and $A_{\rm C}$ are the charge and mass of the compound nucleus, whereas, $Z_{\rm F}$ and $A_{\rm F}$ are the charge and mass of the fission system. $Z_{\rm UCD}$ is the most probable charge based on the unchanged charge-density distribution as suggested by Sugarman and Turkevich [67]. A is the mass of the fission product, whereas $\nu_{\rm pre}$ and $\nu_{\rm post}$ are pre- and postfission neutrons. $\Delta Z_{\rm P}$ ($Z_{\rm P} - Z_{\rm UCD}$) is the charge-polarization parameter. The $+$ and $-$ signs for the $\Delta Z_{\rm P}$ value are applicable to light and heavy fragments, respectively.

The pre- ($\upsilon_{\rm pre}$) and post-scission ($\upsilon_{\rm post}$) neutrons can be calculated as [66]

$$\upsilon_{\rm pre} = \frac{E^*}{7.5 \pm 0.5} + \frac{Z_C^2}{2A_C} - (19.0 \pm 0.5), \quad (6a)$$

$$\upsilon_{\rm post} = \begin{cases} 1.0 \quad \text{for } A > 88 \\ 1.0 + 0.1(A-88) \quad \text{for } 78 < A < 88 \\ 0 \quad \text{for } A < 78. \end{cases} \quad (6b)$$

$Z_{\rm UCD}$ as a function of mass number for the fission product was calculated by using the above equations. On the other hand, the $\Delta Z_{\rm P}$ value can be obtained from the following relation [64]:

$$\Delta Z_{\rm P} = 0 \text{ for } I\eta - 0.5I < 0.04, \quad (7a)$$

$$\Delta Z_{\rm P} = (20/3)(I\eta - 0.5I - 0.04) \quad \text{for} \quad 0.04 < I\eta - 0.5I < 0.085. \quad (7b)$$

The $Z_{\rm P}$ value as a function of mass number was calculated by using Eqs. (5)–(7). The $Y_{\rm FCY}$ values with the average width parameter ($\langle\sigma_z\rangle$) of 0.7 were calculated by using Eq. (3) with the obtained $Z_{\rm P}$ values. The $Y_{\rm FCY}$ values of most fission products in the present work are above 0.9 except for fission products ^{128}Sn, ^{131}Sb, and ^{134}Te, where there is slight difference were observed. The mass-chain yield (Y_A) of the fission products from their relative cumulative yield ($Y_{\rm R}$) was obtained from Eq. (4) by using the $Y_{\rm FCY}$ values of different fission products. The relative mass-chain yields of the fission products obtained as mentioned above were normalized to a total yield of 200% to obtain the absolute mass-chain yields. The absolute cumulative yields of the fission products in the 45- and 80-MeV bremsstrahlung-induced fission of ^{232}Th then were obtained by using the mass-yield data and $Y_{\rm FCY}$ values.

The relative cumulative yield ($Y_{\rm R}$) and mass-chain yield (Y_A) of the fission products in the 45- and 80-MeV bremsstrahlung-induced fission of ^{232}Th along with the nuclear spectroscopic data from Refs. [61,62] are given in Tables I and II, respectively. The absolute mass-chain yields in the above fissioning system from the present work also are given in the last column of Tables I and II, respectively. The uncertainty shown in the measured cumulative yield of individual fission products in Tables I and II is the statistical fluctuation of the mean value from two determinations. The overall uncertainty represents contributions from both random and systematic errors. The random error in the observed activity is due to counting statistics and is estimated to be 10%–15%, which can be determined by accumulating the data for the optimum period of time, depending on the half-life of the nuclide of interest. Conversely, the systematic errors are due to the uncertainties in irradiation time (2%), detector efficiency calibration (~3%), half-life of the fission products (~1%), and γ-ray abundance (~2%), which are the largest variation in the literature [61,62]. Thus, the overall systematic error is about 4%. An upper limit of error of 11%–16% was determined at for the fission-product yields based on 10%–15% random error and a 4% systematic error.

TABLE I. Nuclear spectroscopic data and yields of fission products in the 45-MeV bremsstrahlung-induced fission of ^{232}Th.

Nuclide	Half-life	γ-ray energy (keV)	γ-ray abundance (%)	Y_R (%)[a]	Y_A (%)
^{77}Ge	11.3 h	264.4	54.0	0.378 ± 0.026	0.378 ± 0.026
		416.3	21.8	0.404 ± 0.030	0.404 ± 0.030
^{78}Ge	88.0 min	277.3	96.0	0.562 ± 0.156	0.563 ± 0.156
^{84}Br	31.8 min	1616.2	6.2	4.731 ± 0.437	4.731 ± 0.437
^{85}Kr^{m}	4.48 h	151.2	75.0	4.650 ± 0.130	4.650 ± 0.130
		304.9	14.0	4.442 ± 0.330	4.442 ± 0.330
^{87}Kr	76.3 min	402.6	49.6	4.067 ± 0.439	4.087 ± 0.441
^{88}Kr	2.84 h	196.3	25.9	4.402 ± 0.260	4.520 ± 0.267
^{89}Rb	15.2 min	1032.1	58.0	6.001 ± 0.262	6.013 ± 0.263
		1248.3	42.6	5.746 ± 0.248	5.758 ± 0.248
^{91}Sr	9.63 h	749.8	23.6	4.515 ± 0.300	4.520 ± 0.300
		1024.3	33.0	4.548 ± 0.456	4.553 ± 0.456
^{92}Sr	2.71 h	1384.9	90.0	3.960 ± 0.295	3.972 ± 0.296
^{93}Y	10.18 h	266.9	7.3	3.761 ± 0.363	3.761 ± 0.363
^{94}Y	18.7 min	918.7	56.0	4.298 ± 0.330	4.302 ± 0.330
^{95}Zr	64.02 d	756.7	54.0	4.635 ± 0.522	4.635 ± 0.522
		724.3	44.2	5.039 ± 0.489	5.039 ± 0.489
^{97}Zr	16.91 h	743.4	93.0	4.194 ± 0.070	4.198 ± 0.070
^{99}Mo	65.94 h	140.5	89.4	2.779 ± 0.363	2.779 ± 0.363
		739.5	12.13	2.742 ± 0.330	2.742 ± 0.363
^{101}Mo	14.61 min	590.1	16.4	1.912 ± 0.152	1.912 ± 0.152
^{103}Ru	39.26 d	497.1	90.0	1.251 ± 0.220	1.252 ± 0.220
^{104}Tc	18.3 min	358.0	89.0	1.030 ± 0.152	1.030 ± 0.152
^{105}Ru	4.44 h	724.4	47.0	0.677 ± 0.104	0.678 ± 0.104
^{105}Rh	35.36 h	319.1	19.2	0.785 ± 0.107	0.785 ± 0.107
^{107}Rh	21.7 min	302.8	66.0	0.756 ± 0.152	0.756 ± 0.152
^{112}Ag	3.13 h	617.5	43.0	0.993 ± 0.226	0.993 ± 0.226
^{115}Cd^{g}	53.46 h	336.2	45.9	1.067 ± 0.133	1.067 ± 0.133
^{117}Cd^{m}	3.36 h	1066.0	23.1	0.256 ± 0.019	
^{117}Cd^{g}	2.49 h	273.4	28.0	0.722 ± 0.104	
^{117}Cd^{total}				0.978 ± 0.104	0.978 ± 0.104
^{127}Sb	3.85 d	687.0	37.0	1.025 ± 0.167	1.026 ± 0.167
^{128}Sn	59.07 min	482.3	59.0	1.129 ± 0.063	1.260 ± 0.070
^{129}Sb	4.32 h	812.4	43.0	1.245 ± 0.103	1.467 ± 0.104
^{131}Sb	23.03 min	943.4	47.0	2.062 ± 0.084	2.362 ± 0.096
^{131}I	8.02 d	364.5	81.7	2.734 ± 0.104	2.734 ± 0.104
^{132}Te	3.2 d	228.1	88.0	3.315 ± 0.284	3.372 ± 0.289
^{133}I	20.8 h	529.9	87.0	4.060 ± 0.341	4.060 ± 0.341
^{134}Te	41.8 min	566.0	18.0	3.840 ± 0.373	4.539 ± 0.441
		767.2	29.5	4.316 ± 0.301	5.102 ± 0.356
^{134}I	52.5 min	847.0	95.4	5.239 ± 0.461	5.265 ± 0.463
		884.1	65.0	5.198 ± 0.686	5.224 ± 0.689
^{135}I	6.57 h	1131.5	22.7	3.707 ± 0.040	3.790 ± 0.041
		1260.4	28.9	3.757 ± 0.210	3.842 ± 0.215
^{138}Xe	14.08 min	258.4	31.5	5.319 ± 0.679	5.483 ± 0.700
		434.5	20.3	4.938 ± 0.331	5.091 ± 0.341
^{138}Cs^{g}	33.41 min	1435.8	76.3	6.658 ± 0.167	6.665 ± 0.167
		1009.8	29.8	6.555 ± 0.666	6.562 ± 0.667
		462.8	30.7	6.692 ± 0.267	6.699 ± 0.267
^{139}Ba	83.03 min	165.8	23.7	5.287 ± 0.437	5.287 ± 0.437
^{140}Ba	12.75 d	537.3	24.4	4.579 ± 0.445	4.579 ± 0.445
^{141}Ce	32.5 d	145.4	48.0	4.289 ± 0.366	4.298 ± 0.367
^{142}Ba	10.6 min	255.3	20.5	4.196 ± 0.299	4.209 ± 0.300
^{142}La	91.1 min	641.3	47.0	4.865 ± 0.478	4.865 ± 0.478
^{143}Ce	33.03 h	293.3	42.8	4.946 ± 0.144	4.946 ± 0.144
^{144}Ce	284.89 d	133.5	11.09	5.306 ± 0.508	5.306 ± 0.508

TABLE I. (*Continued.*)

Nuclide	Half-life	γ-ray energy (keV)	γ-ray abundance (%)	Y_R (%)	Y_A (%)
^{146}Ce	13.52 min	316.7	56.0	2.570 ± 0.432	2.575 ± 0.433
		218.2	20.6	2.936 ± 0.477	2.942 ± 0.478
^{146}Pr	24.15 min	453.9	48.0	3.546 ± 0.563	3.546 ± 0.563
		1524.7	15.6	3.401 ± 0.415	3.401 ± 0.415
^{147}Nd	10.98 d	531.0	13.1	3.154 ± 0.378	3.154 ± 0.378
^{149}Nd	1.728 h	211.3	25.9	1.505 ± 0.314	1.508 ± 0.315
		270.2	10.6	1.601 ± 0.358	1.604 ± 0.358
^{149}Pm	53.08 h	286.0	3.1	1.689 ± 0.167	1.689 ± 0.167
^{153}Sm	46.28 h	103.2	30.0	0.330 ± 0.037	0.330 ± 0.037

[a] Y_R is cumulative yields, Y_A is mass yields, ^{135}I is fission rate monitor.

TABLE II. Nuclear spectroscopic data and yields of fission products in the 80-MeV bremsstrahlung-induced fission of ^{232}Th.

Nuclide	Half-life	γ-ray energy (keV)	γ-ray abundance (%)	Y_R (%)[a]	Y_A (%)
^{77}Ge	11.3 h	264.4	54.0	0.399 ± 0.060	0.399 ± 0.060
		416.3	21.8	0.436 ± 0.090	0.436 ± 0.090
^{78}Ge	88.0 min	277.3	96.0	0.559 ± 0.071	0.560 ± 0.071
^{84}Br	31.8 min	1616.2	6.2	4.845 ± 0.154	4.855 ± 0.154
^{85}Kr^{m}	4.48 h	151.2	75.0	4.344 ± 0.136	4.344 ± 0.636
		304.9	14.0	4.340 ± 0.572	4.340 ± 0.572
^{87}Kr	76.3 min	402.6	49.6	4.109 ± 0.221	4.130 ± 0.222
^{88}Kr	2.84 h	196.3	25.9	4.008 ± 0.165	4.111 ± 0.169
^{89}Rb	15.2 min	1032.1	58.0	5.480 ± 0.390	5.491 ± 0.391
		1248.3	42.6	5.266 ± 0.582	5.277 ± 0.583
^{91}Sr	9.63 h	749.8	23.6	4.881 ± 0.406	4.886 ± 0.406
		1024.3	33.0	4.580 ± 0.421	4.585 ± 0.421
^{92}Sr	2.71 h	1384.9	90.0	4.065 ± 0.199	4.077 ± 0.199
^{93}Y	10.18 h	266.9	7.3	3.893 ± 0.391	3.893 ± 0.391
^{94}Y	18.7 min	918.7	56.0	4.140 ± 0.278	4.145 ± 0.278
^{95}Zr	64.02 d	756.7	54.0	5.145 ± 0.286	5.145 ± 0.286
		724.3	44.2	5.269 ± 0.120	5.269 ± 0.120
^{97}Zr	16.91 h	743.4	93.0	4.486 ± 0.462	4.491 ± 0.463
^{99}Mo	65.94 h	140.5	89.4	2.809 ± 0.222	2.809 ± 0.222
		739.5	12.13	2.727 ± 0.150	2.727 ± 0.150
^{101}Mo	14.61 min	590.1	16.4	1.956 ± 0.222	1.956 ± 0.222
^{103}Ru	39.26 d	497.1	90.0	1.191 ± 0.177	1.192 ± 0.177
^{104}Tc	18.3 min	358.0	89.0	1.087 ± 0.075	1.087 ± 0.075
^{105}Ru	4.44 h	724.4	47.0	0.815 ± 0.060	0.816 ± 0.060
^{105}Rh	35.36 h	319.1	19.2	0.997 ± 0.128	0.997 ± 0.128
^{107}Rh	21.7 min	302.8	66.0	0.967 ± 0.241	0.967 ± 0.241
^{112}Ag	3.13 h	617.5	43.0	1.091 ± 0.207	1.091 ± 0.207
^{115}Cd^{g}	53.46 h	336.2	45.9	1.290 ± 0.203	1.290 ± 0.203
^{117}Cd^{m}	3.36 h	1066.0	23.1	0.417 ± 0.105	
^{117}Cd^{g}	2.49 h	273.4	28.0	0.613 ± 0.041	
^{117}Cd^{total}				1.031 ± 0.113	1.031 ± 0.113
^{127}Sb	3.85 d	687.0	37.0	1.274 ± 0.304	1.275 ± 0.305
^{128}Sn	59.07 min	482.3	59.0	1.407 ± 0.152	1.565 ± 0.169
^{129}Sb	4.32 h	812.4	43.0	1.936 ± 0.178	1.959 ± 0.181
^{131}Sb	23.03 min	943.4	47.0	2.444 ± 0.241	2.787 ± 0.275
^{131}I	8.02 d	364.5	81.7	3.159 ± 0.087	3.159 ± 0.087
^{132}Te	3.2 d	228.1	88.0	3.482 ± 0.222	3.539 ± 0.226
^{133}I	20.8 h	529.9	87.0	4.317 ± 0.601	4.321 ± 0.602

TABLE II. (*Continued.*)

Nuclide	Half-life	γ-ray energy (keV)	γ-ray abundance (%)	Y_R (%)	Y_A (%)
^{134}Te	41.8 min	566.0	18.0	4.375 ± 0.298	5.141 ± 0.350
		767.2	29.5	4.321 ± 0.525	5.077 ± 0.617
^{134}I	52.5 min	847.0	95.4	5.370 ± 0.647	5.397 ± 0.651
		884.1	65.0	5.078 ± 0.670	5.104 ± 0.673
^{135}I	6.57 h	1131.5	22.7	3.759 ± 0.037	3.840 ± 0.038
		1260.4	28.9	3.881 ± 0.158	3.964 ± 0.162
^{138}Xe	14.08 min	258.4	31.5	4.979 ± 0.173	5.924 ± 0.579
		434.5	20.3	4.698 ± 0.210	4.799 ± 0.214
^{138}Cs^{g}	33.41 min	1435.8	76.3	5.918 ± 0.579	5.924 ± 0.579
		1009.8	29.8	5.621 ± 0.759	5.626 ± 0.760
		462.8	30.7	6.143 ± 0.323	6.149 ± 0.323
^{139}Ba	83.03 min	165.8	23.7	4.555 ± 0.184	4.555 ± 0.184
^{140}Ba	12.75 d	537.3	24.4	4.318 ± 0.602	4.318 ± 0.602
^{141}Ba	18.27 min	190.3	46.0	4.069 ± 0.255	4.077 ± 0.256
		304.7	35.4	4.185 ± 0.424	4.194 ± 0.425
^{141}Ce	32.5 d	145.4	48.0	4.509 ± 0.316	4.509 ± 0.316
^{142}Ba	10.6 min	255.3	20.5	4.256 ± 0.536	4.269 ± 0.538
		895.2	13.9	4.650 ± 0.296	4.664 ± 0.297
^{142}La	91.1 min	641.3	47.0	4.780 ± 0.530	4.780 ± 0.530
^{143}Ce	33.03 h	293.3	42.8	4.949 ± 0.147	4.949 ± 0.147
^{144}Ce	284.89 d	133.5	11.09	5.059 ± 0.440	5.059 ± 0.440
^{146}Ce	13.52 min	218.2	20.6	3.144 ± 0.120	3.144 ± 0.120
^{146}Pr	24.15 min	453.9	48.0	3.697 ± 0.440	3.697 ± 0.440
		1524.7	15.6	3.475 ± 0.094	3.475 ± 0.094
^{147}Nd	10.98 d	531.0	13.1	3.130 ± 0.346	3.133 ± 0.346
^{149}Nd	1.728 h	211.3	25.9	1.304 ± 0.094	1.309 ± 0.094
		270.2	10.6	1.214 ± 0.330	1.219 ± 0.331
^{149}Pm	53.08 h	286.0	3.1	1.557 ± 0.365	1.557 ± 0.365
^{153}Sm	46.28 h	103.2	30.0	0.353 ± 0.011	0.354 ± 0.011

[a] Y_R is cumulative yields, Y_A is mass yields, ^{135}I is fission rate monitor.

IV. DISCUSSION

The yields of fission products shown in Tables I and II for 45- and 80-MeV bremsstrahlung-induced fission of ^{232}Th from the present paper are determined. The mass-chain-yield data in the bremsstrahlung-induced fission of ^{232}Th at endpoint energy of 45 and 80 MeV from the present paper and those at 10, 25, and 60 MeV from the literature [33,37,38] are plotted in Fig. 1. There is a well-known third peak around the symmetric mass region in the mass-chain-yield distribution of 10–80 MeV bremsstrahlung-induced fission of ^{232}Th as shown in Fig. 1, which is similar to ^{232}Th(n,f) [13–21]. It can be also seen from Fig. 1 that the yields of fission products for A = 133–134, 138–139, and 143–144, and their complementary products are higher than those of the other fission products. A similar observation was shown by us in the neutron-induced fission of various actinides [11,12], in the 10-MeV bremsstrahlung-induced fission of ^{232}Th, ^{238}U, and ^{240}Pu [38], and in the 50–70 MeV bremsstrahlung-induced fission of ^{232}Th [37]. Piessens *et al.* [36] and Pommé *et al.* [50] also observed the similar tendency in the bremsstrahlung-induced fission of ^{232}Th and ^{238}U in the energy region of 6.1–13.1 MeV. The higher yields of fission products for A = 133–134, 138–139, and 143–144 and their complementary products are due to the corresponding even numbers of Z of 52, 54, and 56, respectively [36–38,63]. The oscillation of fission-product yields in the interval of five mass units is due to the A/Z value of about 2.5 for fission products and fissioning systems. Thus the higher yields of the fission products observed around

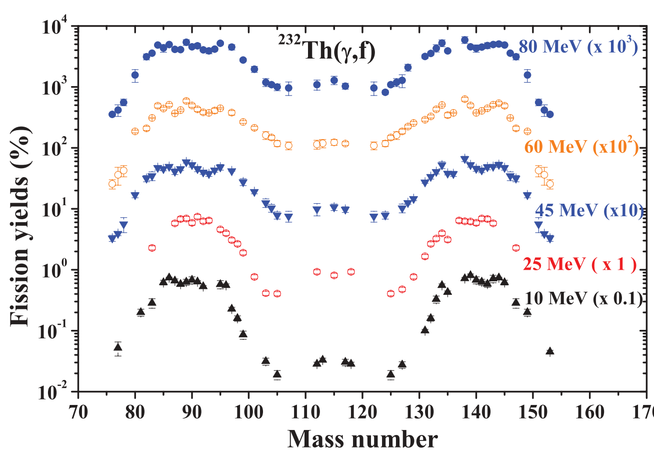

FIG. 1. (Color online) Yields of fission products (%) as a function of mass number in 10-, 25-, 45-, 60-, and 80-MeV bremsstrahlung-induced fission of ^{232}Th. Fission yields for each data are multiplied by numbers written in the plot.

mass numbers of 133–134, 138–139, and 143–144 and their complementary products in the interval of five mass units is most probably due to the even-odd effect of the fragment charge yields as mentioned earlier [68–70]. The effect of the even-odd effect on the mass-yield distribution has been explained in the neutron- [11,12] and bremsstrahlung-induced [38] fission of different actinides. The observation on fine structures in the asymmetric component around mass numbers 133–134 and 143–144 for even-Z fissioning can also be explained from the point of view of the standard I and standard II asymmetric fission modes mentioned by Brossa *et al.* [71], which arise due to shell effects [72]. Based on standard I asymmetry, the fissioning system is characterized by spherical heavy fragment mass numbers 133–134 due to the spherical $82n$ shell and a deformed complementary light mass number. Based on standard II asymmetry, the fissioning system is characterized by a deformed heavy-mass fragment near mass numbers of 143–144 due to a deformed 86–$88n$ shell and slightly deformed light mass. Thus, the higher yields of fission products for $A = 133$–134 and 143–144 are due to the presence of spherical $82n$ and deformed 86–$88n$ shells, respectively. However, shell and pairing effects decrease with an increase in excitation energy for both neutron- [8–21] and bremsstrahlung-induced [30–38] fissions of ^{232}Th.

In order to examine the role of excitation energy, the yields of fission products for $A = 133$–134, $A = 138$–139, and $A = 143$–144 in the bremsstrahlung-induced fission of $^{232}\mathrm{Th}(\gamma,f)$ at different energies from the present work and from other results [30–38,66] are given in Table III. The yields of fission products for $A = 134$, 139, and 143 in $^{232}\mathrm{Th}(\gamma,f)$ from Table III and literature data from $^{232}\mathrm{Th}(n,f)$ [13–21] at different excitation energies are plotted in Fig. 2. It can

TABLE III. Yields of asymmetric (Y_a) products in percent for mass number 133–134, 138–139, and 143–144 in bremsstrahlung-induced fission of ^{232}Th.

E_γ (MeV)	E^* (MeV)	$A = 133$–134	$A = 138$–139	$A = 143$–144	Ref.
6.50	6.02	4.073 ± 0.204	6.257 ± 0.313	8.609 ± 0.431	[63]
		3.819 ± 0.191	7.104 ± 0.355	8.366 ± 0.418	[63]
7.00	6.23	3.301 ± 0.165	7.185 ± 0.359	8.435 ± 0.422	[63]
		4.233 ± 0.212	6.603 ± 0.204	7.657 ± 0.383	[63]
8.0 (7.33)	6.52 (6.34)	3.160 ± 0.158	6.075 ± 0.304	8.005 ± 0.400	[36,63]
		4.652 ± 0.233	7.287 ± 0.364	7.087 ± 0.350	[36,63]
9.0 (8.35)	6.86 (6.64)	3.220 ± 0.180	6.090 ± 0.500	8.530 ± 0.410	[34,36]
		4.900 ± 0.204	6.620 ± 0.710		[34,36]
10.0	7.35	3.275 ± 0.441	7.171 ± 0.306	7.114 ± 0.984	[38]
		5.165 ± 0.400	8.086 ± 0.432	7.414 ± 0.165	[38]
11.0	7.75	3.138 ± 0.157	7.045 ± 0.352	8.249 ± 0.412	[63]
		5.163 ± 0.258	7.480 ± 0.374	8.766 ± 0.438	[63]
12.0 (11.13)	8.35 (7.84)	3.324 ± 0.166	6.851 ± 0.343	7.091 ± 0.355	[36,63]
		4.862 ± 0.243	7.252 ± 0.363	7.779 ± 0.389	[36,63]
14.0	9.44	4.993 ± 0.250	7.156 ± 0.358	6.974 ± 0.349	[36,63]
		5.408 ± 0.270	7.462 ± 0.373	6.558 ± 0.328	[36,63]
15.0	10.5	4.530 ± 0.250	6.000 ± 0.540	7.810 ± 0.370	[34]
			6.700 ± 0.770		[34]
25.0	13.22	3.250 ± 0.260		7.440 ± 0.595	[33]
		3.970 ± 0.318	6.870 ± 0.550	5.800 ± 0.464	[33]
30.0	13.75	3.970 ± 0.318		7.350 ± 0.588	[33]
		3.630 ± 0.290	6.250 ± 0.500	6.020 ± 0.482	[33]
35.0	14.7	4.090 ± 0.327		7.810 ± 0.625	[33]
		3.750 ± 0.300	6.060 ± 0.485	6.410 ± 0.513	[33]
38.0	15.39	5.610 ± 0.370	7.160 ± 0.760	7.300 ± 0.420	[34]
			6.750 ± 0.700		[34]
40.0	15.87	4.130 ± 0.330		5.870 ± 0.470	[33]
		3.760 ± 0.301	5.970 ± 0.478	6.268 ± 0.502	[33]
45.0	16.95	4.064 ± 0.341	6.642 ± 0.367	4.946 ± 0.144	This paper
		5.033 ± 0.336	5.287 ± 0.437	5.306 ± 0.508	This paper
50.0	17.86	4.253 ± 0.087	6.390 ± 0.134	4.726 ± 0.151	[37]
		4.994 ± 0.067	5.702 ± 0.151	4.800 ± 0.174	[37]
60.0	19.76	4.319 ± 0.286	6.287 ± 0.454	5.080 ± 0.269	[37]
		5.036 ± 0.130	4.955 ± 0.313	5.382 ± 0.316	[37]
70.0	21.25	4.137 ± 0.167	6.366 ± 0.199	4.170 ± 0.137	[37]
		5.191 ± 0.242	5.438 ± 0.330	4.891 ± 0.127	[37]
80.0	22.49	4.321 ± 0.602	5.901 ± 0.554	4.949 ± 0.440	This paper
		5.180 ± 0.147	4.555 ± 0.184	5.059 ± 0.440	This paper

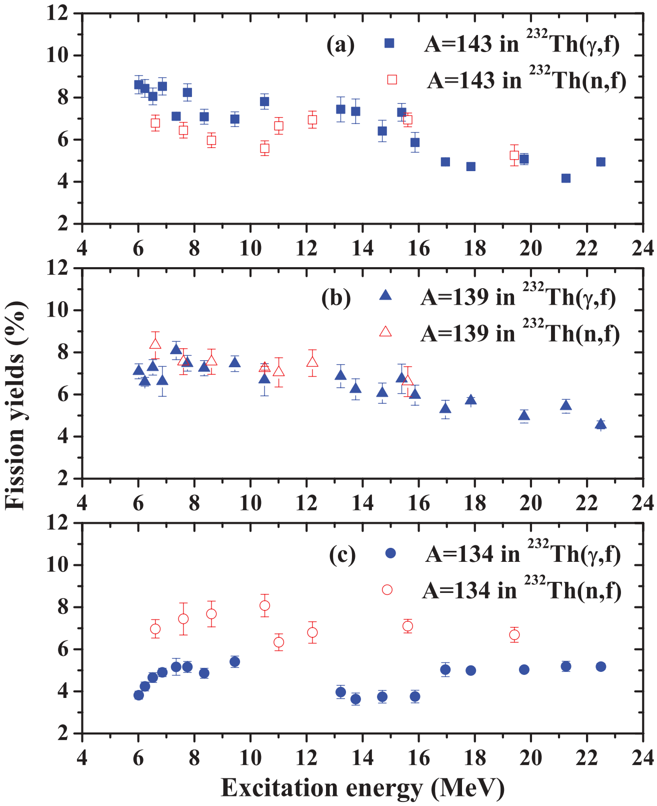

FIG. 2. (Color online) Yields of fission products (%) as a function of excitation energy for (a) $A = 143$, (b) $A = 139$, and (c) $A = 134$ in the ^{232}Th(γ,f) and ^{232}Th(n,f) reactions.

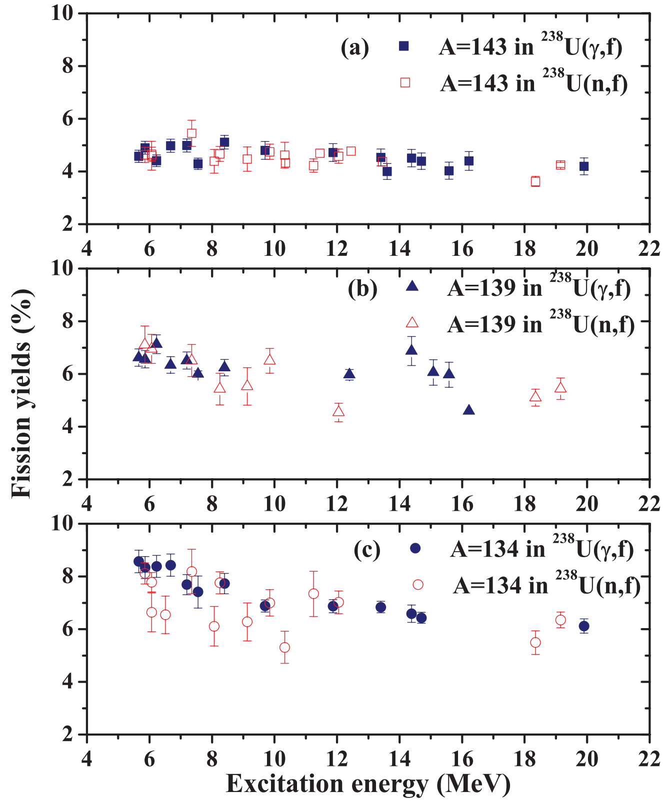

FIG. 3. (Color online) Yields of fission products (%) as a function of excitation energy for (a) $A = 143$, (b) $A = 139$, and (c) $A = 134$ in the ^{238}U(γ,f) and ^{238}U(n,f) reactions.

be seen from Table III that the yields of fission products for $A = 133$–134 increases from 4% at an excitation energy of 6.02 MeV to 5.1% at 22.49 MeV. For mass numbers 138 and 139, the yields of fission products at all excitation energy decreases slightly or remains constant around 6%. On the other hand, for mass numbers 143 and 144, the yields of fission products decrease significantly from 8.6% at 6.02 MeV to 5% at 22.49 MeV. This is to conserve the total yield of 200% for the mass-yields distribution. This observation indicates two different trend of spherical 82n and deformed 86–88n shells of the standard I and standard II asymmetric mode of fission [71] in ^{232}Th. From Fig. 2, it can be seen that, at all excitation energies, the yields of fission products for $A = 133$–134 in ^{232}Th(γ,f) are significantly lower than in ^{232}Th(n,f). On the other hand, the yields of fission products for $A = 143$–144 in ^{232}Th(γ,f) are comparable with those in ^{232}Th(n,f). For fission products at $A = 138$–139, their yields are comparable in both ^{232}Th(γ,f) and ^{232}Th(n,f). In order to examine these aspects in uranium, the yields of fission products for $A = 133$–134, 138–139, and 143–144 in ^{238}U(n,f) [22–29] and in ^{238}U(γ,f) [39–52], as a function of excitation energy, are plotted in Fig. 3. It can be seen from Fig. 3 that the distributions of fission yields in all three mass-chain regions (i.e., $A = 133$–134, 138–139, and 143–144) for the fissioning systems ^{238}U(γ,f) and ^{238}U(n,f) behave almost identically. Thus the different behavior in between ^{232}Th(γ,f) and ^{232}Th(n,f) cannot be explained only from the point of standard I and standard II asymmetric modes of fission [71] based on spherical 82n and deformed 86–88n shell of the heavy fragments unless the potential barrier is considered.

In order to examine the role of excitation energy, the average values of light mass ($\langle A_L\rangle$) and heavy mass ($\langle A_H\rangle$) in the bremsstrahlung-induced fission of ^{232}Th from the present paper with 45- and 80-MeV as well as other lower-energy regions [30–38] are calculated from the mass-chain yields (Y_A) of the fission products within the mass ranges of 80–105 and 125–150, and by using the following relation [47]:

$$\langle A_L\rangle = \sum (Y_A A_L)\Big/\sum Y_A, \quad \langle A_H\rangle = \sum (Y_A A_H)\Big/\sum Y_A. \tag{8}$$

The $\langle A_L\rangle$ and $\langle A_H\rangle$ values obtained from the above relation in the bremsstrahlung-induced fission of ^{232}Th along with their corresponding average excitation energy ($\langle E^*\rangle$) are given in Table IV. From the compound nucleus mass ($A_C = 232$), and from the $\langle A_L\rangle$ and the $\langle A_H\rangle$ values, the experimental average number of neutrons ($\langle v\rangle_{\text{expt}}$) was calculated from the following relation [36]:

$$\langle v\rangle_{\text{expt}} = A_C - (\langle A_L\rangle + \langle A_H\rangle). \tag{9}$$

The $\langle v\rangle_{\text{expt}}$ values obtained from the above relation in the bremsstrahlung-induced fission of ^{232}Th at different excitation energies are listed in Table IV. The $\langle v\rangle$ value at different excitation energies was calculated by Piessens *et al.* [36] assuming the average energy needed for the emission of

TABLE IV. Average light mass ($\langle A_L \rangle$), heavy mass ($\langle A_H \rangle$), and average neutron numbers ($\langle v \rangle_{expt}$ and $\langle v \rangle_{calc}$) in bremsstrahlung-induced fission of ^{232}Th.

E_γ (MeV)	E^* (MeV)	$\langle A_L \rangle$	$\langle A_H \rangle$	$\langle v \rangle_{expt}$	$\langle v \rangle_{calc}$	Ref.
6.44	5.99	88.73 ± 0.11	141.19 ± 0.12	2.08 ± 0.17	2.15	[36]
7.33	6.34	89.06 ± 0.12	140.67 ± 0.12	2.27 ± 0.17	2.16	[36]
8.35	6.64	89.24 ± 0.12	140.53 ± 0.13	2.21 ± 0.18	2.18	[36]
9.31	6.97	89.46 ± 0.12	140.37 ± 0.13	2.15 ± 0.18	2.21	[36]
10.0	7.35	89.62 ± 0.16	140.13 ± 0.15	2.25 ± 0.15	2.25	[38]
11.13	7.75	89.88 ± 0.13	139.91 ± 0.13	2.21 ± 0.19	2.28	[36]
13.15	8.96	90.26 ± 0.14	139.47 ± 0.14	2.27 ± 0.20	2.42	[36]
25.0	13.22	90.39 ± 0.14	138.98 ± 0.15	2.63 ± 0.15	2.82	[33]
30.0	13.75	90.41 ± 0.23	138.95 ± 0.15	2.64 ± 0.19	2.88	[33]
35.0	14.7	90.43 ± 0.14	138.80 ± 0.14	2.77 ± 0.14	2.99	[33]
40.0	15.87	90.66 ± 0.14	138.56 ± 0.15	2.78 ± 0.15	3.12	[33]
45.0	16.95	90.85 ± 0.08	138.41 ± 0.27	2.74 ± 0.18	3.25	This paper
50.0	17.86	91.14 ± 0.14	138.05 ± 0.21	2.81 ± 0.18	3.36	[37]
60.0	19.76	91.32 ± 0.19	137.61 ± 0.19	3.07 ± 0.19	3.58	[37]
70.0	21.25	91.46 ± 0.22	137.32 ± 0.24	3.22 ± 0.23	3.75	[37]
80.0	22.49	91.74 ± 0.25	136.75 ± 0.14	3.50 ± 0.20	3.89	This paper

neutron is 8.6 MeV [73]. The total excitation energy ($\langle E^*_{tot} \rangle$) at the scission point used in the calculation of average neutron numbers ($\langle v \rangle_{calc}$) is obtained from the average Q value ($\langle Q \rangle$), average kinetic energy ($\langle E_K \rangle$), and average excitation energy ($\langle E^* \rangle$) as follows [36]:

$$\langle E^*_{tot} \rangle = \langle Q \rangle - \langle E_K \rangle + \langle E^* \rangle. \tag{10}$$

From Piessens *et al.* [36], we can see that the difference between $\langle Q \rangle$ and $\langle E_K \rangle$ is around 11–12 MeV throughout the bremsstrahlung energy region from 6.5 to 13.15 MeV. Since an $\langle E_K \rangle$ value in the bremsstrahlung energy higher than 13.15 MeV is not available in the literature, the difference between $\langle Q \rangle$ and $\langle E_K \rangle$ is used as 11 MeV for the bremsstrahlung energy higher than 13.15 MeV. The $\langle v \rangle_{calc}$ value obtained based on the above assumption is listed in Table IV. The $\langle v \rangle_{expt}$ values for ^{232}Th(γ,f) from Table IV and those for ^{232}Th(n,f) reaction from Ref. [20] are plotted in Fig. 4(a). Similarly, the $\langle v \rangle_{expt}$ values for ^{238}U(γ,f) [37,38] and those for ^{238}U(n,f) [28,29] are plotted in Fig. 4(b) for comparison. It can be seen from Fig. 4 that in both bremsstrahlung- and neutron-induced fission of ^{232}Th and ^{238}U, the values of $\langle v \rangle_{expt}$ increase with excitation energy. However, from Fig. 4, it can be seen that, at the same excitation energy, the $\langle v \rangle_{expt}$ values for ^{232}Th(n,f) are higher than those for ^{232}Th(γ,f) unlike the similar value between ^{238}U(γ,f) and ^{238}U(n,f). For the same excitation energy, the lower values of $\langle v \rangle_{expt}$ in ^{232}Th(γ,f) compared to ^{232}Th(n,f) may be due to the different type of potential-energy surface and/or outer fission barrier between them.

The $\langle A_L \rangle$ and $\langle A_H \rangle$ values for the ^{232}Th(γ,f) reaction from Table IV and those for the ^{232}Th(n,f) reaction from Ref. [20] are plotted in Fig. 5. Similarly, the $\langle A_L \rangle$ and the $\langle A_H \rangle$ values for the ^{238}U(γ,f) reaction from Refs. [37,38] and those for the ^{238}U(n,f) reaction from Refs. [28,29] are plotted in Fig. 6, for comparison. From Fig. 5, it can be seen that the $\langle A_H \rangle$ values for both the ^{232}Th(γ,f) and the ^{232}Th(n,f) reactions decreases with the excitation energy, whereas, the $\langle A_L \rangle$ values increases with the excitation energy. However, at all excitation energy, the $\langle A_H \rangle$ values for the ^{232}Th(γ,f) reaction are slightly higher than those for the ^{232}Th(n,f) reaction and the $\langle A_L \rangle$ values for the ^{232}Th(γ,f) reaction are significantly lower than those for the ^{232}Th(n,f) reaction, as seen in Fig. 5. This is due to the mass conservation based on the standard I and II asymmetric mode of fission.

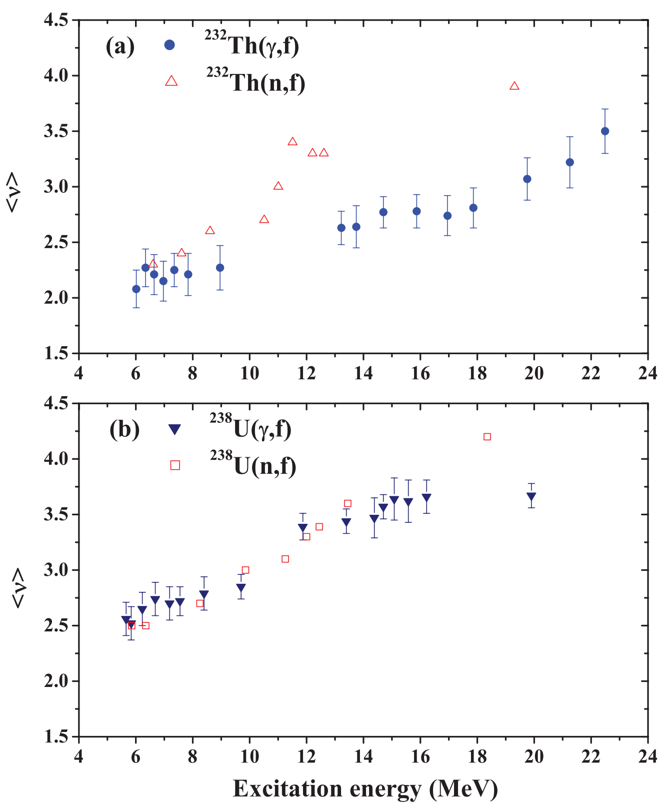

FIG. 4. (Color online) Measured average neutron number as a function of excitation energy (a) in the ^{232}Th(γ,f) and ^{232}Th(n,f) reactions and (b) in the ^{238}U(γ,f) and ^{238}U(n,f) reactions.

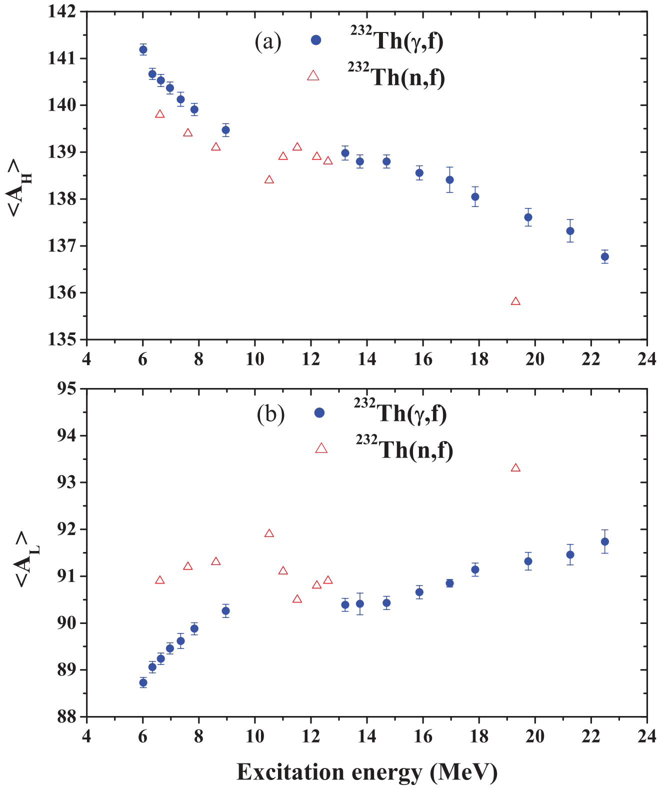

FIG. 5. (Color online) (a) Average values of heavy mass ($\langle A_{\mathrm{H}}\rangle$) and (b) average values of light mass ($\langle A_{\mathrm{L}}\rangle$) as a function of excitation energy in the ^{232}Th(γ,f) and ^{232}Th(n,f) reactions.

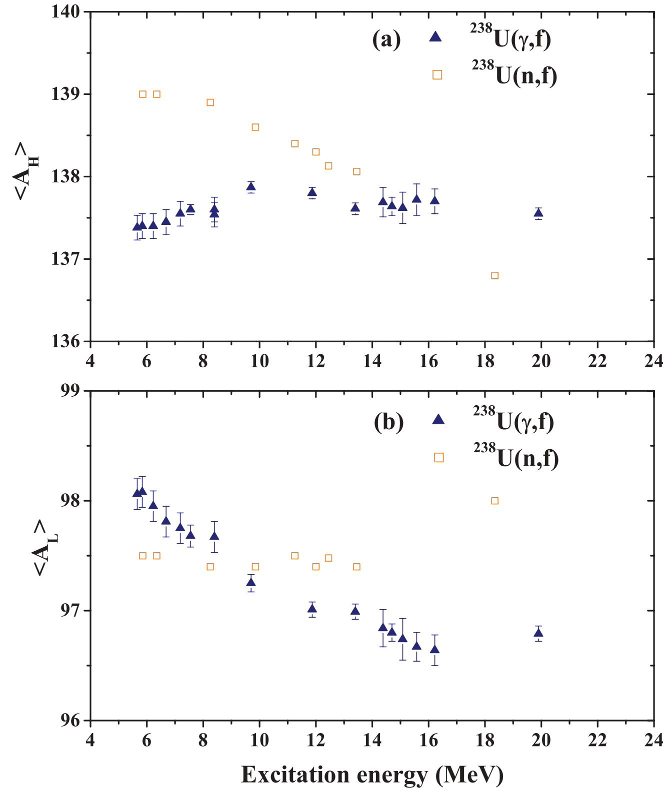

FIG. 6. (Color online) (a) Average values of heavy mass ($\langle A_{\mathrm{H}}\rangle$) and (b) average values of light mass ($\langle A_{\mathrm{L}}\rangle$) as a function of excitation energy in the ^{238}U(γ,f) and ^{238}U(n,f) reactions.

From Fig. 6, it can be seen that the $\langle A_{\mathrm{H}}\rangle$ values for the ^{238}U(γ,f) reaction and the $\langle A_{\mathrm{L}}\rangle$ values for the ^{238}U(n,f) increases with the excitation energy, whereas, that the $\langle A_{\mathrm{H}}\rangle$ values for the ^{238}U(n,f) reaction and the $\langle A_{\mathrm{L}}\rangle$ values for the ^{238}U(γ,f) decreases with the excitation energy. The increase or decrease trend of the $\langle A_{\mathrm{L}}\rangle$ and $\langle A_{\mathrm{H}}\rangle$ values with excitation energy in ^{238}U(γ,f) and ^{238}U(n,f) is due to the mass conservation based on standard I and II asymmetric mode of fission. However, the different behavior of the $\langle A_{\mathrm{L}}\rangle$ and $\langle A_{\mathrm{H}}\rangle$ values with excitation energy in the ^{238}U(γ,f) reaction compared to ^{238}U(n,f), ^{232}Th(n,f), and ^{232}Th(γ,f) is due to the interplay of standard I and II asymmetric mode of fission [71] based on the shell combination [72] of the complementary products [11,12,37,38], besides the role of excitation energy.

In order to examine the role of potential energy barrier, the yield of fission products in the peak position for the asymmetric products, those in the valley region for the symmetric products, and their ratios [i.e., peak-to-valley (P/V) ratio] in the bremsstrahlung-induced fission of ^{232}Th at 45 and 80 MeV from the present paper and other energy regions [36–38,63] are given in Table V. The experimental yield of symmetric and asymmetric fission products as well as the P/V ratios for ^{232}Th(γ,f) from Table V and for ^{232}Th(n,f) from the literature data [13–21], as a function of excitation energy, are shown in Figs. 7 and 9, respectively. Similarly, the experimental yield of symmetric and asymmetric fission products as well as the P/V ratios for ^{238}U(n,f) [22–29] and ^{238}U(γ,f) [39–52] are also plotted in Figs. 8 and 10 for comparison. From Figs. 7 and 8, it can be seen that the yields of asymmetric fission products decrease marginally with an increase in excitation energy, whereas, the yield of symmetric products increases sharply up to 8 MeV where second-chance fission starts. Thereafter, the increasing trend is slow with an increase in the excitation energy. This is because, when the excitation energy exceeds the neutron binding-energy of the compound nucleus, second-chance fission starts where fission occurs from the residual nucleus at lower excitation energy. The number of prefission neutron emissions also increases with an increase of excitation energy. Thereby, the small part of the total excitation energy will be available in the fission degrees of freedom as the intrinsic excitation energy. This causes the slow increase in the yields of fission products resulting in the slow decrease in the P/V ratio with an increase in excitation energy as shown in Figs. 9 and 10. However, the increasing trend of the symmetric yields and the decreasing trend of the P/V ratio are sharper in the ^{232}Th(γ,f) reaction compared to those in the ^{238}U(γ,f) reaction. A similar observation was reported in our previous papers [37,38] in both the bremsstrahlung- and the neutron-induced fission of ^{232}Th and ^{238}U. Furthermore, it can be seen from Figs. 9 and 10 as well as from our previous work [37,38] that the P/V ratios in the bremsstrahlung- and the neutron-induced fission of ^{232}Th are always lower than those of ^{238}U and other actinides. This observation is due to the different type of potential barrier in ^{232}Th compared to that in ^{238}U as shown by Moller [74], who calculated

TABLE V. Yields of asymmetric (Y_a) and symmetric (Y_s) products and P/V ratio in bremsstrahlung-induced fission of ^{232}Th.

E_γ (MeV)	E^* (MeV)	Y_a (%)[a]	Y_s(%)	P/V ratio	Ref.
6.50	6.02	8.609 ± 0.431			[63]
7.00	6.23	8.435 ± 0.422			[63]
8.0 (7.33)	6.52 (6.34)	8.005 ± 0.400	<0.008	696.1 ± 214.7	[36,63]
			<0.015		[36]
9.0 (8.35)	6.86 (6.64)	8.530 ± 0.410	0.090 ± 0.030	85.3 ± 21.7	[34,36]
			0.110 ± 0.020		[36]
9.31	6.97	(8.308 ± 0.415)	0.250 ± 0.050	38.6 ± 6.6	[36]
			0.180 ± 0.020		[36]
10.0	7.35	8.086 ± 0.432	0.304 ± 0.032	26.6 ± 3.5	[38]
11.0	7.75	8.766 ± 0.438			[63]
12.0 (11.13)	8.35 (7.84)	7.779 ± 0.389	0.650 ± 0.100	13.5 ± 1.9	[36,63]
			0.500 ± 0.020		[36]
14.0	9.44	7.852 ± 0.393	(0.725 ± 0.036)	10.8 ± 0.8	[36,63]
15.0	10.5	7.890 ± 0.610	(0.810 ± 0.041)	9.7 ± 0.9	[34,36]
25.0	13.22	7.440 ± 0.595	0.813 ± 0.065	8.0	[33]
25.0	13.22		0.870 ± 0.120		[31]
30.0	13.75	7.350 ± 0.588	0.871 ± 0.070	7.6	[33]
35.0	14.7	7.810 ± 0.625	0.905 ± 0.072	6.9	[33]
38.0	15.39	7.300 ± 0.420			[34]
40.0	15.87	7.280 ± 0.582	0.904 ± 0.072	6.6	[33]
45.0	16.95	6.642 ± 0.367	1.067 ± 0.133	6.2 ± 0.8	This paper
50.0	17.86	6.448 ± 0.128	1.218 ± 0.188	5.3 ± 0.8	[37]
60.0	19.76	6.287 ± 0.032	1.235 ± 0.131	5.1 ± 0.5	[37]
69.0	21.24	6.800 ± 0.499	(1.364 ± 0.120)	5.0 ± 0.6	[30]
70.0	21.25	6.366 ± 0.154	1.364 ± 0.120	4.7 ± 0.4	[37]
80.0	22.49	5.900 ± 0.554	1.290 ± 0.203	4.6 ± 0.8	This paper

[a]Yield of fission product given in brackets is extrapolated value from references.

the saddle-point configurations against the mass asymmetric deformation. This has been proven by Yoneama *et al.* [75] using electrofission (i.e., the virtual photon-induced fission of ^{232}Th). As mentioned by them [75], the outer barrier in ^{232}Th splits into two barriers with heights of 6.5 and

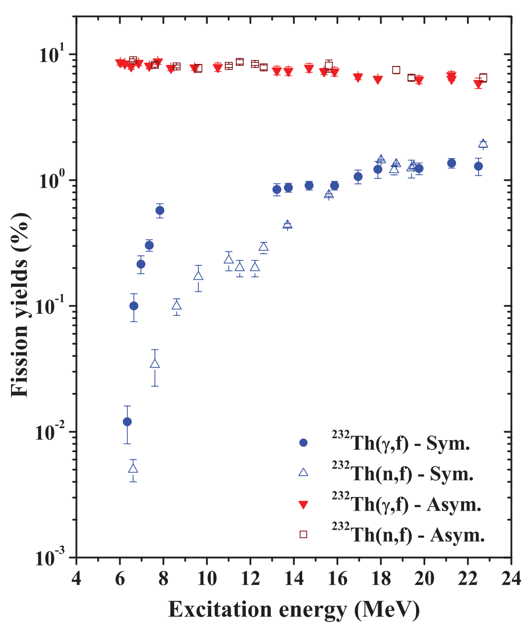

FIG. 7. (Color online) Yields of symmetric and asymmetric fission products (%) in bremsstrahlung- and neutron-induced fission of ^{232}Th as a function of excitation energy.

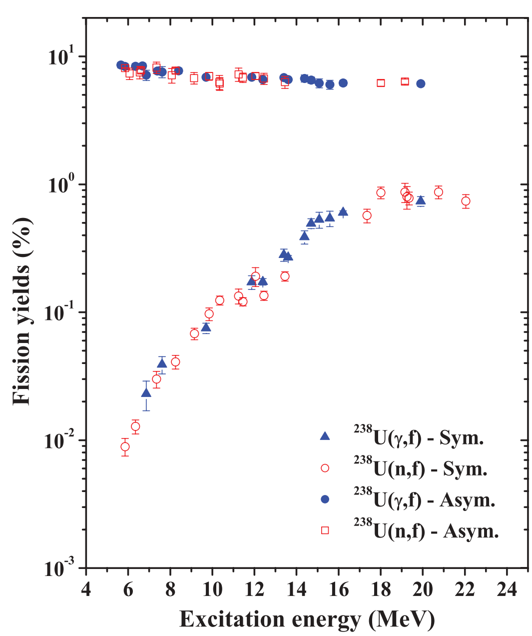

FIG. 8. (Color online) Yields of symmetric and asymmetric fission products (%) in bremsstrahlung- and neutron-induced fission of ^{238}U as a function of excitation energy.

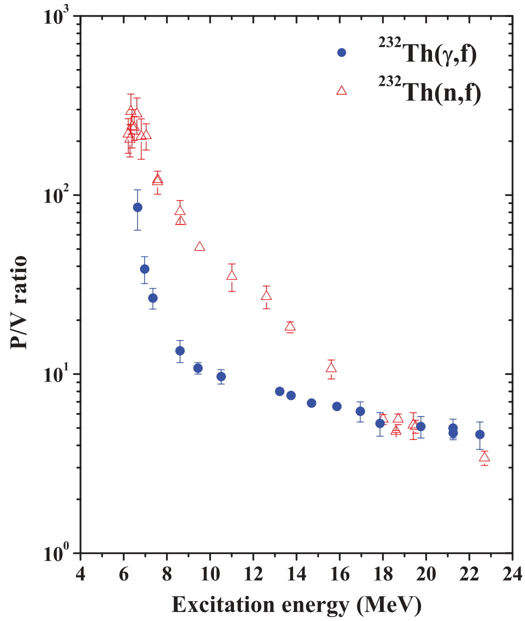

FIG. 9. (Color online) Peak-to-valley (P/V) ratio as a function of excitation energy in bremsstrahlung- and neutron-induced fission of ^{232}Th.

5.7 MeV separated by a shallow minimum with a bottom at 5.4 MeV. They have also shown that the barrier height changes for the different vibrational states. The calculation of saddle-point configurations against the mass asymmetric deformation by Moller [74] showed a different type of potential barrier for ^{232}Th compared to ^{238}U. Thus, the observation of a triple-humped mass distribution from the present and earlier

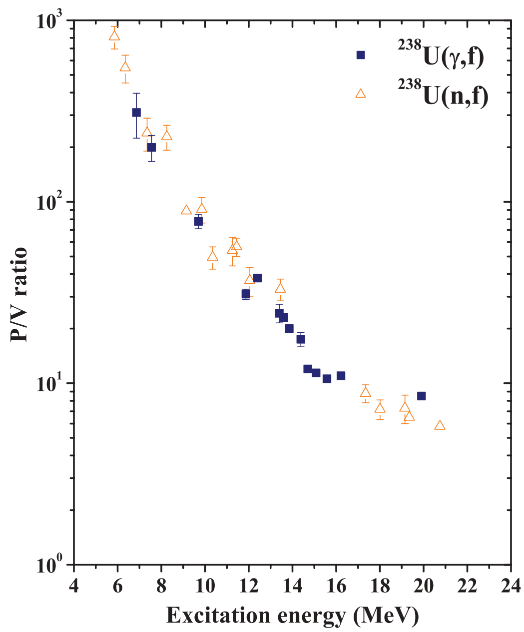

FIG. 10. (Color online) Peak-to-valley (P/V) ratio as a function of excitation energy in bremsstrahlung- and neutron-induced fission of ^{238}U.

work in bremsstrahlung- [30–38], reactor neutron- [8–10], and mono-energetic neutron-induced [13–21] fission of ^{232}Th compared to that of ^{238}U is due to a different type of potential barrier.

Furthermore, it is observed that the increase of symmetric products yields (Fig. 7) and decrease of P/V ratios (Fig. 9) are sharper in ^{232}Th(γ,f) than in ^{232}Th(n,f). However, in the case of ^{238}U(γ,f) and ^{238}U(n,f), increase of symmetric products yields (Fig. 8) and decrease of P/V ratios (Fig. 10) follows a similar trend. Even the absolute yield value of symmetric fission products (Fig. 8) and P/V ratios (Fig. 10) are comparable at the same excitation energy for ^{238}U(γ,f) and ^{238}U(n,f) systems. The surprising difference of symmetric products (Fig. 7) and P/V ratios (Fig. 9) between ^{232}Th(γ,f) and ^{232}Th(n,f) may be due to the different type of potential barrier in the fissioning system ^{232}Th* compared to ^{233}Th* and/or due to the lower fission barrier in ^{232}Th* than in ^{233}Th* [60,74]. At lower excitation energy, this may cause the availability of lower energies in the intrinsic degree of freedom in ^{233}Th* than in ^{232}Th* depending upon the nuclear viscosity (i.e., coupling between collective and intrinsic degrees of freedom). This is clearly reflected in the even-odd effect in the bremsstrahlung- [61,62] and neutron-induced [68] fissions of ^{232}Th and ^{238}U. These observations indicate the role of excitation energy in addition to the qualitative picture of sharing excitation energy between the intrinsic and the collective degrees of freedom depending on nuclear viscosity, which is different for different actinides.

V. CONCLUSIONS

(i) The yields of fission products in the 45- and 80-MeV bremsstrahlung-induced fission of ^{232}Th were determined by using an offline γ-ray spectrometric technique. The mass-yield distributions in the ^{232}Th(γ,f) reaction at various energies are triple humped, similar to those of the ^{232}Th(n,f) reaction.

(ii) The yields of fission products for $A = 133$–134, $A = 138$–139, and $A = 143$–144 and their complementary products in the bremsstrahlung-induced fission of ^{232}Th are higher than those of other fission products. This is due to nuclear structure such as the role of shell closure proximity based on standard I and II asymmetric mode of fission in addition to the even-odd effect.

(iii) The yields of fission products for $A = 133$–134 and their complementary products in the ^{232}Th(γ,f) reaction are lower than those in the ^{232}Th(n,f) reaction, whereas, those for $A = 143$–144 and their complementary products are reversed. This indicates the different role of standard I and II asymmetric mode of fission.

(iv) The yields of asymmetric products in the ^{232}Th(γ,f) and the ^{232}Th(n,f) reactions, marginally decreased with increasing the excitation energy. The yields of symmetric products increased sharply up to the excitation energy of 8 MeV and, thereafter, it varied slowly due to an increase in the prefission neutron emission and the multichance fission probability. Thus, we observed the decreasing trend in the P/V ratio with increasing excitation energy.

(v) The increasing trend of the symmetric product yields and the decreasing trend of the peak-to-valley (P/V) ratio as a function of excitation energies in the ^{232}Th(γ,f) reaction is faster than in ^{232}Th(n,f). Besides this, the yields of symmetric products are higher and the value of the P/V ratio is lower in ^{232}Th(γ,f) than in ^{232}Th(n,f), unlike in ^{238}U(γ,f) and ^{238}U(n,f) within the excitation energy of 16 MeV. This may be due to the different type of potential barrier for ^{232}Th* compared to ^{233}Th*.

(vi) In bremsstrahlung- and neutron-induced fission of ^{232}Th and ^{238}U, the values of $\langle v\rangle_{\text{expt}}$ increase with increasing excitation energy. However, at the same excitation energy, the values of $\langle v\rangle_{\text{expt}}$ are higher in ^{232}Th(n,f) than in ^{232}Th(γ,f) unlike the similar value in between ^{238}U(γ,f) and ^{238}U(n,f). This may be due to lower outer fission barrier in the fissioning system ^{232}Th* than in ^{233}Th*.

ACKNOWLEDGMENTS

The authors express their sincere thanks to the staff of the PAL for the excellent operation of the electron linac and their support during the experiment. This research was partly supported by the National Research Foundation of Korea (NRF) through a grant provided by the Korean Ministry of Education, Science & Technology (MEST) in 2011 (Project No. 2011-0006306 and No. 2011-0025762), by the World Class University (WCU) program (Grant No. R31-30005), by Kyungpook National University Research Fund, 2012, and by the Institutional Activity Program of Korea Atomic Energy Research Institute. One of the authors (H. Naik) thanks to Dr. K. L. Ramakumar for supporting the program and for permitting him to visit PAL, Korea to carry out this experiment.

[1] C. Wagemans, *The Nuclear Fission Process* (CRC, London, 1990).
[2] R. Vandenbosch and J. R. Huizenga, *Nuclear Fission* (Academic, New York, 1973).
[3] E. A. C. Crouch, At. Data Nucl. Data Tables **39**, 417 (1977).
[4] A. C. Wahl, At. Data Nucl. Data Tables **39**, 1 (1988).
[5] B. F. Rider, Compilation of Fission Products Yields, Vallecitos Nuclear Center Report NEDO-12154-3c, General Electric Co., USA, 1981 (unpublished).
[6] T. R. England and B. F. Rider, Evaluation and Compilation of Fission Products Yields, ENDF-349, LA-UR-94-3106, 1993 (unpublished).
[7] M. James and R. Mills, Neutron Fission Products Yields, JEF-2.2, 1993 (unpublished).
[8] H. N. Erten, A. Gruetter, E. Rossler, and H. R. von Gunten, Nucl. Sci. Eng. **79**, 167 (1981).
[9] R. H. Iyer, C. K. Mathews, N. Ravindran, K. Rengan, D. V. Singh, M. V. Ramaniah, and H. D. Sharma, J. Inorg. Nucl. Chem. **25**, 465 (1963).
[10] A. Turkevich and J. B. Niday, Phys. Rev. **84**, 52 (1951).
[11] H. Naik, A. G. C. Nair, P. C. Kalsi, A. K. Pandey, R. J. Singh, A. Ramaswami, and R. H. Iyer, Radiochimica Acta **75**, 69 (1996).
[12] R. H. Iyer, H. Naik, A. K. Pandey, P. C. Kalsi, R. J. Singh, A. Ramaswami, and A. G. C. Nair, Nucl. Sci. Eng. **135**, 227 (2000).
[13] K. M. Broom, Phys. Rev. **133**, B874 (1964).
[14] R. Ganapathy and P. K. Kuroda, J. Inorg. Nucl. Chem. **28**, 2017 (1966).
[15] T. Mo and M. N. Rao, J. Inorg. Nucl. Chem. **30**, 345 (1968).
[16] M. Thein, M. N. Rao, and P. K. Kuroda, J. Inorg. Nucl. Chem. **30**, 1145 (1968).
[17] L. H. Gevaert, R. E. Jervis, and H. D. Sharma, Can. J. Chem. **48**, 641 (1970).
[18] D. L. Swindle, D. T. Moore, J. N. Beck, and P. K. Kuroda, J. Inorg. Nucl. Chem. **33**, 3643 (1971).
[19] J. Trochon, H. A. Yehia, F. Brisard, and Y. Pranal, Nucl. Phys. A **318**, 63 (1979).
[20] L. E. Glendenin, J. E. Gindler, I. Ahmad, D. J. Henderson, and J. W. Meadows, Phys. Rev. C **22**, 152 (1980).
[21] S. T. Lam, L. L. Yu, H. W. Fielding, W. K. Dawson, and G. C. Neilson, Phys. Rev. C **28**, 1212 (1983).
[22] J. T. Harvey, D. E. Adams, W. D. James, J. N. Beck, J. L. Meaon, and P. K. Kuroda, J. Inorg. Nucl. Chem. **37**, 2243 (1975).
[23] D. R. Nethaway and B. Mendoza, Phys. Rev. C **6**, 1827 (1972).
[24] D. E. Adams, W. D. James, J. N. Beck, and P. K. Kuroda, J. Inorg. Nucl. Chem. **37**, 419 (1975).
[25] M. Rajagopalan, H. S. Pruys, A. Grutter, E. A. Hermes, and H. R. von Gunten, J. Inorg. Nucl. Chem. **38**, 351 (1976).
[26] W. D. James, D. E. Adams, J. N. Beck, and P. K. Kuroda, J. Inorg. Nucl. Chem. **37**, 1341 (1975).
[27] T. C. Chapman, G. A. Anzelon, G. C. Spitale, and D. R. Nethaway, Phys. Rev. C **17**, 1089 (1978).
[28] S. Nagy, K. F. Flynn, J. E. Gindler, J. W. Meadows, and L. E. Glendenin, Phys. Rev. C **17**, 163 (1978).
[29] A. Afarideh and K. R. Annole, Ann. Nucl. Energy **16**, 313 (1989).
[30] D. M. Hiller and D. S. Martin, Jr., Phys. Rev. **90**, 581 (1953).
[31] L. H. Gevaert, R. E. Jervis, S. C. Subbarao, and H. D. Sharma, Can. J. Chem. **48**, 652 (1970).
[32] B. Schrøder, G. Nydahl, and B. Forkman, Nucl. Phys. A **143**, 449 (1970).
[33] A. Chattopadhyay, K. A. Dost, I. Krajbich, and H. D. Sharma, J. Inorg. Nucl. Chem. **35**, 2621 (1973).
[34] J. C. Hogan, A. E. Richardson, J. L. Meason, and H. L. Wright, Phys. Rev. C **16**, 2296 (1977).
[35] W. Gunther, K. Huber, U. Kneissl, H. Krieger, and H. J. Maier, Z. Phys. A **295**, 333 (1980).
[36] M. Piessens, E. Jacobs, S. Pommé, and D. De Frenne, Nucl. Phys. A **556**, 88 (1993).
[37] H. Naik, T. N. Nathaniel, A. Goswami, G. N. Kim, M. W. Lee, S. V. Suryanarayana, S. Ganesan, E. A. Kim, M. H. Cho, and K. L. Ramakumar, Phys. Rev. C **85**, 024623 (2012).
[38] H. Naik, V. T. Nimje, D. Raj, S. V. Suryanarayana, A. Goswami, S. Singh, S. N. Acharya, K. C. Mttal, S. Ganesan, P. Chandrachoodan, V. K. Manchanda, V. Venugopal, and S. Banarjee, Nucl. Phys. A **853**, 1 (2011).
[39] R. A. Schmitt and N. Sugarman, Phys. Rev. **95**, 1260 (1954).
[40] H. G. Richter and C. D. Coryell, Phys. Rev. **95**, 1550 (1954).

[41] L. Katz, T. M. Kavanagh, A. G. W. Cameron, E. C. Bailey, and J. W. T. Spinks, Phys. Rev. **99**, 98 (1958).
[42] J. L. Meason and P. K. Kuroda, Phys. Rev. **142**, 691 (1966).
[43] I. R. Willams, C. B. Fulmer, G. F. Dell, and M. J. Engebretson, Phys. Lett. B **26**, 140 (1968).
[44] D. Swindle, R. Wright, K. Takahashi, W. H. Rivera, and J. L. Meason, Nucl. Sci. Eng. **52**, 466 (1973).
[45] W. D. James, D. E. Adams, R. A. Sigg, J. T. Harvey, J. L. Meason, J. N. Beck, P. K. Kuroda, H. L. Wright, and J. C. Hogan, J. Inorg. Nucl. Chem. **38**, 1109 (1978).
[46] H. Thierens, D. De Frenne, E. Jacobs, A. De Clercq, P. D'hondt, and A. J. Deruytter, Phys. Rev. C **14**, 1058 (1976).
[47] E. Jacobs, H. Thierens, D. De Frenne, A. De Clercq, P. D'hondt, P. De Gelder, and A. J. Deruytter, Phys. Rev. C **19**, 422 (1979).
[48] A. De Clercq, E. Jacobs, D. De Frenne, H. Thierens, P. D'hondt, and A. J. Deruytter, Phys. Rev. C **13**, 1536 (1976).
[49] E. Jacobs, A. De Clercq, H. Thierens, D. De Frenne, P. D'hondt, P. De Gelder, and A. J. Deruytter, Phys. Rev. C **20**, 2249 (1979).
[50] S. Pommé, E. Jacobs, M. Piessens, D. De Frenne, K. Persyn, K. Govaert, and M.-L. Yoneama, Nucl. Phys. A **572**, 237 (1994).
[51] A. Yamadera, T. Kase, and T. Nakamura, in *Proceedings of the International Conference on Nuclear Data for Science and Technology, Moto, Japan, 1988* (Japan Atomic Energy Research Institute, Tokai, Japan, 1988), p. 1147.
[52] A. Göök, M. Chernykh, C. Eekardt, J. Enders, P. von Neumann-Cosel, A. Oberstedt, S. Oberestedt, and A. Richter, Nucl. Phys. A **851**, 1 (2011).
[53] G. N. Kim, H. Ahmed, R. Machrafi, D. Son, V. Skoy, Y. S. Lee, H. Kang, M.-H. Cho, I. S. Ko, and W. Namkunng, J. Korean Phys. Soc. **43**, 479 (2003).
[54] V. D. Nguyen, D. K. Pham, D. T. Tran, V. D. Phung, Y. S. Lee, G. N. Kim, Y. Oh, H. S. Lee, H. Kang, M.-H. Cho, I. S. Ko, and W. Namkung, J. Korean Phys. Soc. **50**, 417 (2007).
[55] S. Agostinelli *et al.* (GEANT4 Collaboration), Nucl. Instrum. Methods A **506**, 250 (2003).
[56] A. I. Blokhin and A. S. Soldatov, Phys. At. Nucl. **72**, 917 (2009).
[57] J. T. Caldwell, E. J. Dowdy, B. L. Berman, R. A. Alvarez, and P. Meyer, Phys. Rev. C **21**, 1215 (1980).
[58] M. Veyssiere, H. Bell, R. Bergere, P. Carlos, A. Lepretre, and K. Kernbath, Nucl. Phys. A **199**, 45 (1973).
[59] A. J. Koning, S. Hilaire, and M. C. Duijvestijn, in *Proceedings of the International Conference on Nuclear Data for Science and Technology*, edited by R. C. Haight, M. B. Chadwick, T. Kawano, and P. Talou, AIP Conf. Proc. No. 769 (AIP, New York, 2005), p. 1154.
[60] S. Bjornholm and J. E. Lynn, Rev. Mod. Phys. **52**, 725 (1980).
[61] E. Browne and R. B. Firestone, in *Table of Radioactive Isotopes*, edited by V. S. Shirley (Wiley, New York, 1986); R. B. Firestone and L. P. Ekstrom, in *Table of Radioactive Isotopes*, Version 2.1 (2004) [http://ie.lbl.gov/toi/index.asp].
[62] J. Blachot and C. Fiche, Ann. Phys. Suppl. **6**, 3 (1981).
[63] K. Persyn, E. Jacobs, S. Pommé, D. De Frenne, K. Govaert, and M.-L. Yoneama, Nucl. Phys. A **620**, 171 (1997).
[64] S. Pommé, E. Jacobs, K. Persyn, D. De Frenne, K. Govaert, and M. L. Yoneama, Nucl. Phys. A **560**, 689 (1993).
[65] D. De Frenne, H. Thierens, B. Proot, E. Jacobs, P. De Gelder, A. De Clercq, and W. Westmeier, Phys. Rev. C **26**, 1356 (1982).
[66] H. Umezawa, S. Baba, and H. Baba, Nucl. Phys. A **160**, 65 (1971).
[67] N. Sugarman and A. Turkevich, in *Radiochemical Studies: The Fission Product*, edited by C. D. Coryell and N. Sugarman, Vol. 3 (Mc Graw-Hill, New York, 1951), p. 1396.
[68] H. Naik, R. J. Singh, and R. H. Iyer, Eur. Phys. J. A **16**, 495 (2003).
[69] H. Naik, R. J. Singh, and R. H. Iyer, J. Phys G: Nucl. Part Phys. **30**, 107 (2004).
[70] H. Naik, S. P. Dange, R. J. Singh, and S. B. Manohar, Nucl. Phys. A **612**, 143 (1997).
[71] U. Brossa, S. Grossmann, and A. Muller, Phys. Rep. **197**, 167 (1990).
[72] B. D. Wilkins, E. P. Steinberg, and R. R. Chasman, Phys. Rev. C **14**, 1832 (1976).
[73] H. Nifenenecker, C. Signabieux, R. Babinet, and J. Poitou, in *Physics and Chemistry of Fission*, Vol. I (IAEA, Vienna, 1973), p. 17.
[74] P. Moller, Nucl. Phys. A **192**, 529 (1972).
[75] M. L. Yoneama, E. Jacobs, J. D. T. Arruda-Neto, B. S. Bhandari, D. De Frenne, S. Pommé, K. Persyn, and K. Govaert, Nucl. Phys. A **604**, 263 (1996).